Fe–Co magnetic nanoclusters by density functional theory calculations

C. S. Cutrano and Ch. E. Lekka

Department of Materials Science and Engineering, University of Ioannina, Ioannina, Greece

ABSTRACT
We present density functional theory results referring to the structural, electronic and magnetic properties of 13, 55, 147 and 309 Fe–Co (magnetic–magnetic) icosahedral nanoclusters (ICO) comparing with our previous results on Fe–Cu (magnetic–nonmagnetic). It came out that the Fe atoms always favour the edge surface sites exhibiting higher average magnetic moment (MM) for Fe and FeCo ICOs than FeCu while the local Fe MM is greater for $FeCu_{12}$ and Fe_6Cu_{49} ones. This is due to the strong hybridisation of Fe $3d$–Co $3d$ states, while in Fe–Cu the Fe spin down states are restricted close to fermi without been affected by the corresponding Cu states. These results could be used for the design of environmental sustainable smart magnetic alloys.

Introduction

Transition metal clusters and coatings are interesting since their structural, electronic and magnetic properties depend on their size and composition, rendering them suitable candidates for various potential applications. In particular, the magnetic moment (MM) of Fe clusters with less than 100 atoms is around 3 μ_B much higher than the corresponding 2.2 μ_B bulk value while it decays as a function of clusters' size towards the bulk values [1–5]. Similar behaviour was also found by density functional theory (DFT) calculations when mixing Fe with a non-magnetic element like Cu in 13, 55, 147 and 309 magic numbered ICO clusters [6]. It is found that the local Fe MM of the $FeCu_{12}$ is almost double than the bulk Fe while the Fe (111) triangle face in $Cu_{49}Fe_6$, $Cu_{137}Fe_{10}$ and $Cu_{294}Fe_{15}$ MM (2.7 μ_B) converges faster to the Fe monolayer (ML) on Cu(111) (2.3–2.7 μ_B) than the Fe at edge positions which nevertheless exhibit the highest local MM (3.1 μ_B) [6].

These DFT data agree with experimental studies that the Fe/Cu(111) MM stands within the large ICOs and the bulk MM values [6–10]. Indeed, when growing Fe thin films on non-magnetic substrates like Cu results in an fcc tetragonal distorted (fct) structure depending on the film thickness showing higher local Fe MM up to 2.5–2.7 μ_B on Cu(100) and 3.3 μ_B on Cu(111) than the Fe bcc (2.1–2.15 μ_B) [7–10]. To this end, experiments on Fe ultrathin ferromagnetic (FM) fcc tetragonal distorted film grown on magnetic fcc Co(100) coherently produced on non-magnetic fcc Cu(100), showed similar structural and thickness dependent magnetic properties [11–14]. The thinnest (up to 4ML) Fe film's MM is 3.0 μ_B on Co(100) and 2.8 μ_B on Cu(100) while between 5 and 10 ML they drop to 1.1 and 0.8 μ_B, respectively [14]. However, the study of Fe's MM on fcc-like Co(111) on Cu(111) to our knowledge is still lacking although the Fe on Cu(111) reveals higherMM than Fe growing on Cu(100) [7–14].

Concerning the nanoclusters, theoreticalDFT calculations on large ICOs (up to 400 atoms) to our knowledge are limited in pure (e.g. Co, Fe and Ni) [3,4,5,15], Co-Mn (13, 55 atoms) [16] and Fe–Cu (13, 55, 147 and 309) [6] nanoclusters. It came out that as the size of the cluster increases, the clusters' MM decreases to the corresponding bulk value; the cluster's core atom MM approaches faster the bulk MM than the cluster's surface MM [3–6]. Experimental results show that Ni clusters' MM with more than 300 atoms approach the bulk limitmore rapidly than the Co and FeMMclusters whichneedmore than500 atoms toconverge [2].Moreover,

Fe$_{55}$ shows an antiferromagnetic (AFM) coupling between the central atom and first shell's atoms while the Fe$_{147}$MMoscillates between the shells fromantiferromagnetic to ferromagnetic [4]. On the contrary, Co$_{55}$ and Co$_{147}$ maintain a ferromagnetic behaviour like Co$_{13}$ [4,5]. Concerning the electronic properties, the clusters up to 55 atoms (Fe, Co, Ni and Fe–Cu) display halfmetallic character in the sense thatHOMO–LUMO energy gap is very small for minority spin as compared to that for majority-spin component while the 147 and 309 icosahedra show metallic nature [4,6]. Nevertheless, studies concerning the electronic and structural properties of clusters having Fe and magnetic element substitutions like Co and sizes higher than 13 atoms, e.g. icosahedral 55, 147 and 309 to our knowledge are absent.

The transition metal clusters with less than 20 atom have been widely studied with *ab initio* calculations [17–26]. DFT revealed that the icosahedral Fe$_{13}$ exhibits the highest MM 3.38 μ_B among all $3d$ and $4d$ transition 13 and 23 atom metal clusters [15] while for Co$_{13}$ and Cu$_{13}$ hcp-like structures are favoured [19]. Moreover, it is found that in Fe$_{12}$X, (X = Al and $3d$ element) the local spin MM of a substituent atom decreases with respect to that substituted iron atom except for the case of surface Mn atom where the local MM is 4.6 μ_B [24,25]. Similarly, in ferromagnetic (Co$_x$Fe$_{1-x}$)$_N$ (N = 5, 13), although the local MM of both Co and Fe atoms is slight enhanced as the Co concentration increases, the average MM decreases since

Co atoms have one less d hole [17]. Interestingly, when doping non-magnetic element clusters like Cu13 with Fe, the local Fe MM becomes almost double than the Fe bcc due to its partially filled 3d shell although antiferromagnetic alignment is found between the Cu and Fe MM [6,26].

In this work, we present a systematic study of Fe–Co icosahedral clusters aiming to reveal the electronic and magnetic properties as well as the evolution of MM towards the FeCo thinnest film onCu(111)which could be considered as an infinite cluster's surface side system. The comparison with the local Fe MM of the Fe–Cu clusters and thin films is also provided using our previous SIESTA calculations [6] and the calculated average clusters' MM in order to understand the influence of a magnetic (Co) and non-magnetic (Cu) substitution in Fe.

Computational details

We performedDFT calculations within the general gradient density approximation of Perdew and Wang [27] using the SIESTA [28]. For all elements, the core electrons were replaced by norm-conserving pseudopotentials in the fully nonlocal Kleinmane Bylander [29] form and the basis set was a linear combination of numerical atomic orbitals constructed from the eigenstates of the atomic pseudopotentials [30]. For the 13-atomcluster we considered the boundary Fe12Co and Co12Fe cases. For the 55-atom we perform a detail configuration investigation, taken into

account the energetically favoured Fe sites, the triangle (111) facets and the edge positions, aiming to depict the system with the highest MM and to compare our data with the Fe-Cu nanoclusters' results. All the understudy 55-atom configurations are in Figure 1 in the next session. In line with the FeCu case, we choose the triangle and edge configuration for the 147 and the 309 clusters. For cases we used a box with vacuum twice as large as the size of the nanocluster in order to avoid periodic images interactions while no – periodic boundary conditions were applied.

The surfaces consist of a (3×3×2) Cu(111) unit cell supercell resulting in six atomic layers with nine atoms. We consider the cases of Fe monolayer on Cu(111), Fe/Co atomic layers on Cu(111), Co/Fe on Cu(111) and mix FeCo on Cu(111) thin films. We applied in-plane periodic boundary conditions and a 9×9×1 k-point mesh. The vacuum spacing is equal to the length of the supercell along [111] direction while the three atomic layers were fixed in order to mimic the bulk behaviour. For the geometry optimisation, the structure is considered fully relaxed when the magnitude of forces on the atoms was smaller than 0.005 eVA$_{-1}$. The cluster's binding energies (Eb) were calculated by subtracting from the clusters total energy the corresponding equal number of Fe and Co atomic energies.

Results and discussion
Structural and magnetic properties

Aiming to reveal theMMmoment evolution as the size of the cluster increases towards (111) thin films and the taken into account the ICO favoured structure of the larger Fe and Co clusters as well as its (111)-like facet which shows the highest MM we adopt for all nanoclusters, even for the tiny 13-atom. Consequently, we started with the smallest 13 atom FeCo cluster and we consider the boundary cases of $Fe_{12}Co$ (E_b is equal to –3.25 and –3.27 eV when Fe is a core atom) and $Co_{12}Fe$ (–3.34 and –3.33 eV for Fe core atom). We found that Co always like to be core atom in line with previous DFT on $Fe_{12}Co$ [24] while the most stable is the $Co_{12}Fe$. The totalMMis higher in the Fe-rich cluster $Fe_{12}Co$ (43.2 μ_B), having the biggest local MM on the Fe shell atom of $Co_{12}Fe$ (3.1 μ_B). The Co core atom exhibits always the lowest MM (1.8 μ_B). These results are in line with our previous calculations on $Cu_{12}Fe$ clusters were the local MM was higher at the Fe shell atom [6]. On the contrary, the $Cu_{12}Fe$ cluster shows antiferromagnetic behaviour between Cu and Fe atoms while in the case of Fe–Cowe always observe ferromagnetic behaviour. The E_b of the Fe_{13} (–3.24 eV) stands within the previous DFT data ranging from –3.07 to –4.43 eV [17], the total MM is 44.1 μ_B (2.6 μ_B/atom) in line with 44 μ_B [17] while the Fe shell atoms show higher MM (3.1 μ_B). In addition, the Co_{13} (–3.33 eV) is compared to binding energies ranging from–3.26 up to –5.14 eV [17] and the local MM at the shell atoms

(2.1 μB) and at the core (1.9 μB) are higher than the bulk value (1.7 μB) in line with previous DFT calculations [4,15,17].

The next magic number for icosahedral clusters is the 55. For these FeCo there are several configurations depending on the Fe composition depicted in Figure 1. Starting with the pure Co_{55} and Fe_{55} icosahedral clusters we found the total MM at 103 and
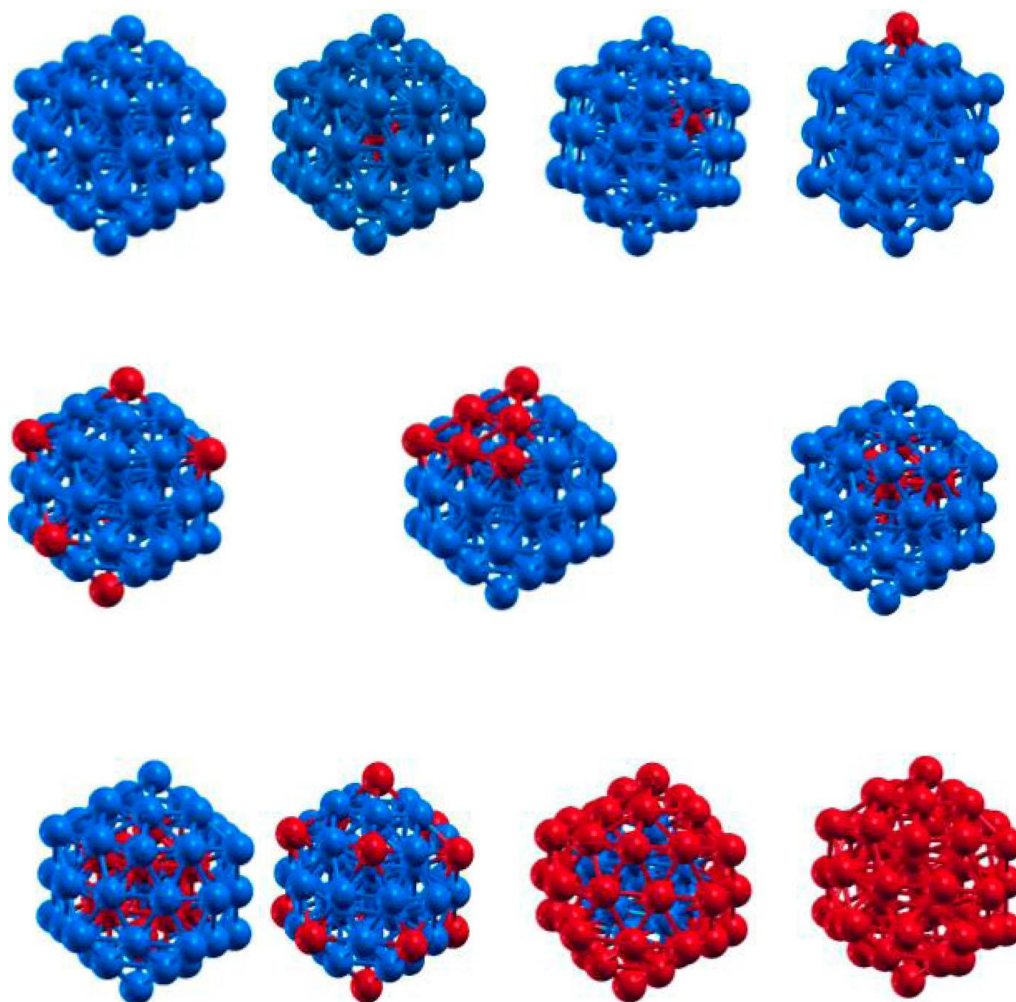

Figure 1. Co–Fe icosahedral 55 atom clusters along with the corresponding local MM and the binding energy. Blue (dark) and red (light) spheres stand for the Co and Fe atoms.

150 μ_B, respectively, in line with 105 and 150 μ_B of [24]. Co$_{55}$ shows a FM behaviour between all cluster's atoms while Fe$_{55}$ displays AFM coupling between core and first shell's atoms. Firstly, we substitute a Fe atom in all available sites of Co$_{55}$ (core, first and surface shell) as presented in Figure 1. It came out that the Co$_{54}$Fe energetically favoured configuration is the one with Fe atom at the clusters' surface which also shows the highest local MM (2.99 μ_B) compared to the other cases. The Co surface atoms of Cu$_{54}$Fe local MM varies from 1.84 to 1.87 μ_B while the core Co atom has on the average 1.6 μ_B that is smaller than the Co bcc (1.7 μ_B). This Fe atom's higher local MM at the surface was also found for the Cu$_{49}$Fe case [6]. Furthermore, we study several configurations in the Co$_{49}$Fe$_6$ clusters by substituting six Co atoms with Fe atoms: (a) at the cluster's edge (–4.163 eV), (b) side (covering one surface side triangle, –4.159 eV) and (c) the half 1rst shell positions (–4.157 eV) revealing the Edge Co$_{49}$Fe$_6$ as the energetically favoured. In addition, the Edge Co$_{49}$Fe$_6$ exhibits the highest local Fe MM (2.92 μ_B) compared to the Side (2.87 μ_B) and 1st shell's (2.50 μ_B) configurations in line with the Cu$_{49}$Fe cases [6]. For theCo$_{49}$Fe$_6$ clusters, theCo surface atoms show local MM up to 1.87 μ_B which decreases at the 1st shell (average 1.70 μ_B) and drops at the Co core atom(1.5–1.6 μ_B) in values lower thantheCo bccwhile the total cluster MM is around 106–108 μ_B. The next composition was the Co$_{43}$Fe$_{12}$ where Fe atoms substitute: (a) all surface edge sites (–4.117 eV) or (b) all the 1st shell positions (–4.126 eV) in line with Co$_{49}$Fe$_6$,

which show again that the Fe located at the edges is the energetically favoured configuration with great Fe local MM(2.91 μB). In the $Co_{43}Fe_{12}$ cases, the Co localMM decreases evenmore at the first shell (1.05 μB) while the core atom retains 1.65 μB. Finally, the $Co_{13}Fe_{42}$ where Fe covers the cluster's surface (–4.368 eV) is favoured against the Fe_{55} (–3.823 eV) showing higher local Fe MM (2.76 μB) in line with $Cu_{13}Fe_{42}$ case [6]. Summarising, we found that in 55 Co–Fe clusters the binding energy decreases as the Fe composition increases while the highest value for the local Fe MM is at the surface edge. For all cases, the Co and Fe reveal FM behaviour while the Cu and Fe clusters show AFM character.

For the 147 clusters, we focused on the $Co_{135}Fe_{12}$ edge configuration having Fe at the edge surface sites and the $Co_{137}Fe_{10}$ where Fe atoms cover the surface triangle side. The edge $Co_{135}Fe_{12}$ (–4.41 eV) is energetically favoured against the $Co_{137}Fe_{10}$ (–4.25 eV).

For the $Co_{135}Fe_{12}$ the total MM is 294 μB while the Fe local MM is 3.00 and 1.82 μB for Co surface atoms. The $Co_{137}Fe_{10}$ triangle case displays greater total MM of 335 μB but lower Fe local MM of 2.89 μB and higher Co local MM 1.90 μB compared to the edge $Co_{135}Fe_{12}$ case. Finally, the Fe and Co atoms reveal FM behaviour in both $Co_{135}Fe_{12}$ and $Co_{137}Fe_{10}$ clusters.

Electronic density of states (EDOS)

Chemical reactivity of metallic clusters depends on the EDOS close to the Fermi level. In this section, we present the total and partial EDOS for the selective cases of (a) $Co_{12}Fe$, (b) $Co_{49}Fe_6$, $Co_{135}Fe_{12}$ when Fe occupies the Edge surface sites and (c) the Fe on Co MLs grown on Cu(111), Figure 2. The first columna
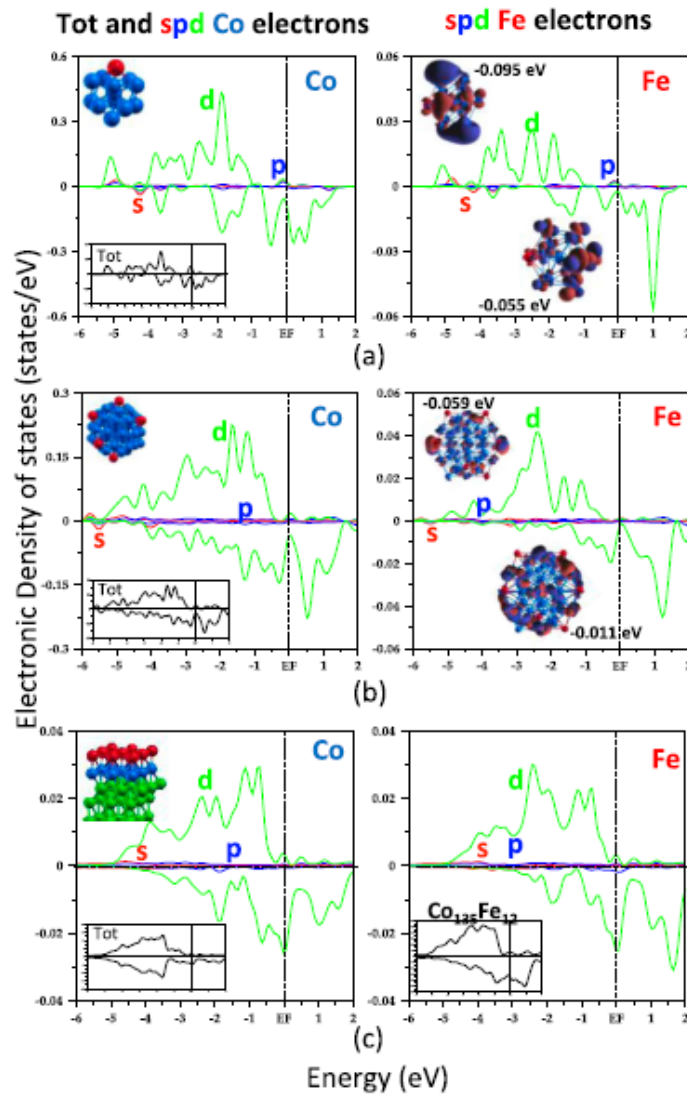
Figure 2. EDOS: (a) Co12 Fe, (b) Co49Fe6 and (c) Fe/CoMLon Cu(111). The spin up and spin downhighest occupiedwavefunctions are depicted for Co12Fe and Co49Fe6. Black, red, blue and green lines stand for the total, s, p and d electrons' contributions, respectively.

while the second column stands for the Fe partial EDOS. The molecular-like $Co_{12}Fe$ EDOSs of both Co and Fe show more localised states which are broadened and become wider as the size of the cluster increases approaching band characteristics of the films on Cu(111). In addition, for all cases the spin majority shows different behaviour than the spin minority revealing the electronic origin of the MM. Both Co and Fe states stand from –6 eV up to the fermi level while the highest occupation is due to the $3d$ electrons rather than the sp. Focusing on the $Co_{12}Fe$ EDOS, both Co and Fe spin up $3d$ states are more localised than the spin down while the spin down state around –0.5 eV and around –2 eV exist in both atoms indicating their enhanced hybridisation. At the fermi level, both d and p orbitals contribute in the spin up states while the spin down states is basically occupied by the d electrons of both atoms. The $Co_{12}Fe$ total EDOS in the inset of Co EDOS clearly shows the different spin up and spin down electron occupation. Comparing with the $Cu_{12}Fe$ EDOS, the more visible difference is the almost empty occupation of the Fe 3d spin down states, showing only a pronounced state around –0.3 eV [6]. In the $Co_{49}Fe_6$ EDOS the spin up Co 3d states are wider while the Fe exhibits a pronounced 3d occupation around –2.eV. The $Co_{49}Fe_6$ spin down 3d EDOS exhibits states from–4 eVup to the fermiwhichgradually increase their occupation while the Fe 3d states are basically located from –2 to –1 eV showing a pseudo gap at the fermi level. The total $Co_{49}Fe_6$ EDOS follows as expected mainly the Co partial EDOS while similar

characteristics shows the Co135Fe12 total spin up EDOSs although more pronounced. In the Co135Fe12 total spin down EDOSs the pseudogap at the fermi level is partially filled due to the Co 3d spin down states. Interestingly, the Co(111) ML on Cu(111) reveals similar Co and Fe spin up states with the Co49Fe6 having only higher occupation around–1 eV. Inthe spindown both Co and Fe 3d states appears around –2 eV and at the fermi level while the spin up fermi level occupancy is almost absent. In the total EDOS CoFe thin film on Cu(111) the Cu states are dominant and therefore the high occupation of the states mainly below –3.5 eV is observed.

MM

In Figure 3, we present the average total MM (a) for the basic under study cases as well as the local Fe MM (b) aiming to reveal the size dependence and the system with the highest values of MM. In Figure 3(a), we observe that the highest averageMMstands for the Fe13 while the Fe-Cu clusters reveal the lowest average MM due to theAFMbehaviour and the almost absentMMat the Cu atoms (dashed line and open symbols are taken from our LSDA – DFT calculations [6]). The Fe–Co clusters saw higherMMthan the pure Co13 and Co55 as well as the Co bcc suggesting the improved MM upon Fe substitution with small MM difference between the 55 and 147 triangle and edge configurations. Turning on the local Fe MM, Figure 3(b), we observe that the Co12Fe, Co49Fe6 and Co135Fe12 clusters show

higher Fe MM than the pure Fe clusters, Fe fcc and Fe
bcc, showing similar MM values for the Edge and triangle
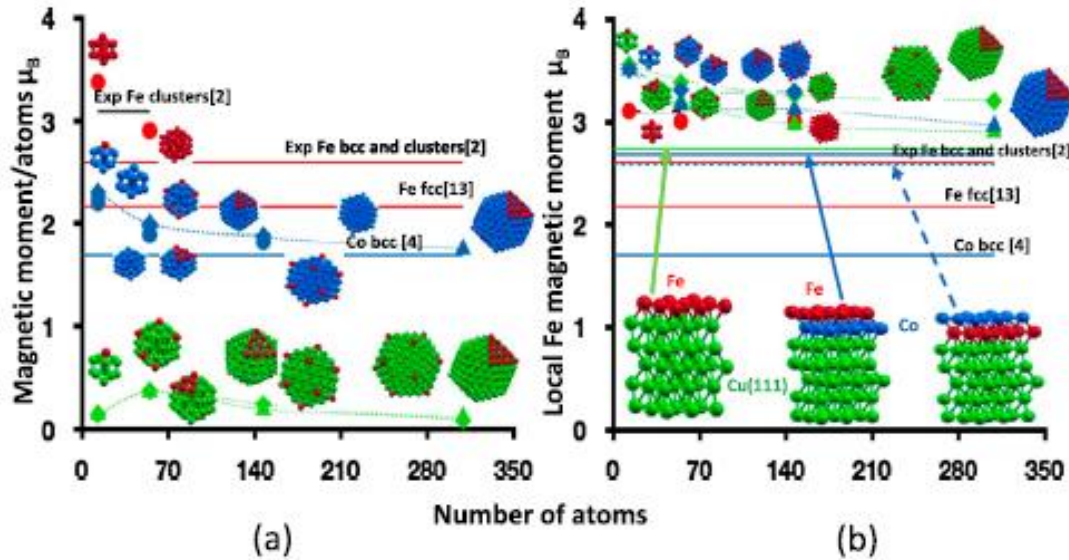cases. In addition, all the Fe–Co clusters reveal

Figure 3. MMper atoms (µB) of the CoFe Edge and Triangle clusters (blue diamond triangle), Fe clusters (red), Fe12Co (violet triangle spilled), CuFe Edge and triangle (green triangle and diamond), CuFe Edge and Triangle calculations [6] (green open diamond and triangle), FeCu(111) (green line), FeCoCu(111) (turquoise line), CoFeCu(111) (turquoise dashed line) Experimental Fe clusters (black line), Fe bcc (red line), Fe fcc (purple line), Co bcc (blue line).

bigger Fe MM compare to the Fe ML on Co or
Cu(111) surface. Finally, it should be noted that Fe local
MM is equivalent between the clean Cu(111) and the
Co/Cu(111) once Fe remains as the outermost surface
layer.

Conclusions

In this work, we present DFT calculations on Fe–Co
and compare our data with Fe–Cu clusters and thin
films aiming to understand the influence of Fe in magneticornon-
magnetic systems. It cameout that bothCo

and Cu atoms always favour the core cluster's site while the Fe atoms the edge surface sites. Fe–Co and Fe–Cu clusters reveal the Edge configuration as the one with the highest Fe local MM. In addition, the $Fe_{12}Co$ shows the greatest MM that converges towards the fcc FeCo (111) thin film as the size of the cluster increases. For all cluster sizes, the Co and Fe reveal FM behaviour while the Cu and Fe clusters show AFM character. The electronic properties reveal that the Fe 3d states are strongly hybridise with the Co 3d for both spin up and spin down EDOS while in the Fe–Cu clusters the Fe partial 3d spin down EDOS is saturated close to the fermi level. The $Co_{12}Fe$ and $Co_{49}Fe_6$ clusters reveal a pseudogap at the fermi level in the spinminority that is altered in the case of $Co_{135}Fe_{12}$ and Fe/Co/Cu(111). Concluding, the FMFe–Co clusters or Fe coating ofCo/Cu(111) are suggested as the best candidate for Fe-based systems with equivalent total and local Fe MM compared to the corresponding Fe–Cu systems. These resultsmight be used for the design of magnetic devices with tune magnetic properties.

Disclosure statement

No potential conflict of interest was reported by the authors.

References

[1] Jena P, Castleman AW. Clusters: a bridge across the disciplines of physics and chemistry. PNAS. 2006;28: 10560–10569. DOI:10.1073/pnas.0601782103.

[2] Billas IML, Chatelain A, de HeerWA. Magnetism from the atom to the bulk in iron, cobalt, and nickel clusters. Science. 1994;265:1682–1684. DOI:10.1126/science. 265.5179.1682.

[3] Tiago ML, Zhou Y, Alemany MMG, et al. Evolution of magnetism in iron from the atom to the bulk. Phys Rev Lett. 2006;97:147201. DOI:10.1103/PhysRevLett.97. 147201.

[4] Singh R, Kroll P. Structural, electronic, and magnetic properties of 13-, 55-, and 147 atom clusters of Fe, Co, and Ni: a spin-polarized density functional study. Phys Rev B. 2008;78:245404.Doi:10.1103/PhysRevB.78. 245404.

[5] Souto-Casares J, Sakurai M, Chelikwsky JR. Structural and magnetic properties of large cobalt clusters. Phys Rev B. 2016;93:174418. DOI:10.1103/PhysRevB.93. 174418.

[6] Cutrano CS, Lekka CE. Structural, magnetic and electronic properties of Cu-Fe nanoclusters by density functional theory calculations. J Alloys Compd. 2017;707:114–119. DOI:10.1016/j.jallcom.2016. 11.425.

[7] Donath M. Magnetic order and electronic structure in thin films. J Phys Condens Matter. 1999;11:9421–9436.

DOI:10.1088/0953-8984/11/48/306.

[8] Choi H, Lee SG, Chung YC. The role of structural variations in the magnetism of Fe/Cu(111): first-principles calculations. Comput Mater Sci. 2010;49:S291–S296. DOI:10.1016/J.commatsci.2010.01.032.

[9] Kish T, Nakamoshi H, Kasai H, et al. Magnetic properties of Fe thin films on Cu(111). J Phys Soc Japan. 2002;71:2983–2985. DOI:10.1143/JPSJ.71.2983.

[10] Moroni EG, Kresse G, Hafner J. Coherent epitaxy and magnetism of face-centered-cubic Fe films on Cu(100). J Phys Condens Matter. 1999;11:L35–L42. DOI:10.1088/0953-8984/11/5/003.

[11] Kamakura N, Kimura A, Saitoh T, et al. Magnetism of Fe films grown on Co(100) studied by spin-resolved Fe 3s photoemission. Phys Rev B. 2006;73:094437. DOI:10.1103/PhysRevB.73.094437.

[12] Escorcia-Aparicio EJ, Kawakami RK, Qiu ZQ. Fcc Fe films grown on a ferromagnetic fcc Co(100) substrate. Phys. Rev. B. 1996;54:4155–4158. doi:10.1103/PhysRevB.54.4155.

[13] Dallmeyer A, Maiti K, Rader O, et al. Magnetism and interlayer coupling in fcc Fe/Co films. Phys. Rev. B. 2001;63:104413. doi:10.1103/PhysRevB.63.104413.

[14] Schmitz D, Charton C, Scholl A, et al. Magnetic moments of fcc Fe overlayers on Cu(100) and Co(100). Phys Rev B. 1999;59:4327–4333. DOI:10.1103/PhysRevB.59.4327.

[15] Aguilera-Grangia F, Garcia-Fuente A, Vega A. Comparative ab initio study of the structural, electronic, and magnetic trends of isoelectronic late 3d and 4d transition metal clusters. Phys Rev B. 2008;78:134425. DOI:10.1103/PhysRevB.78.134425.

[16] Rollman G, Sahoo S, Hucht A, et al. Magnetism and

chemical ordering in binary transition metal clusters. Phys Rev B. 2008;78:134404. DOI:10.1103/PhysRevB. 78.134404.

[17] Aguilera-Granja F, Vega A. Stability,magnetic behavior, and chemical order of $(Co_xFe_{1-x})N$ (N=5,13) nanoalloys. Phys Rev B. 2009;79:144423. DOI:10.1103/Phys RevB.79.144423.

[18] Piotrowski MC, Ungureanu CG, Tereshchuk P, et al. Theoretical study of the structural, energetic, and electronic properties of 55-atommetal nanoclusters: ADFT investigation within van der waals corrections, spinorbit coupling, and PBE+U of 42 metal systems. J Phys Chem C. 2016;120:28844. DOI:10.1021/acs.jpcc. 6b10404.

[19] Piotrowski MJ, Piquini P, Da Silva JLF. Density functional theory investigation of $3d$, $4d$, and $5d$13-atom metal clusters. Phys Rev B. 2010;81:155446. DOI: 10.1103/PhysRevB.81.155446.

[20] Dong CD, Gong XG. Magnetism enhanced layerlike structure of small cobalt clusters. Phys Rev B. 2008;78:020409(R).DOI:10.1103/PhysRevB.78.020409.

[21] Ma M, Xie Z, Wang J, et al. Structures, stabilities and magnetic properties of small Co clusters. Phys Lett A. 2006;358:289. DOI:10.1016/j.physleta.2006. 05.033.

[22] Sun Q, Gong XG, Zeng QQ, et al. Local magnetic properties and electronic structures of $3d$ and $4d$ impurities in Cu clusters. Phys Rev B. 1996;54:10896. DOI:10.1103/PhysRevB.54.10896.

[23] Valkealahti S, Manninen M. Instability of cuboctahedral copper clusters. Phys Rev B. 1992;55:9459. DOI:10.1103/PhysRevB.45.9459.

[24] Gustev GL, Jhonson LE, Belay KG, et al. Structure

and magnetic properties of Fe12X clusters. Chem
Phys. 2014;430:62–68. DOI:10.1016/j.chemphys.2013.
12.014.

[25] Aguilera-Granja F, Longo RC, Gallego LG, et al. Structural
and magnetic properties of X12Y (X, Y=Fe,
Co, Ni, Ru, Rh, Pd and Pt) nanoalloys. J Chem Phys.
2010;132:184507. DOI:10.1063/1.3427292.

[26] Ling W, Dong D, Shi-Jian W, et al. Geometrical, electronic,
and magnetic properties of CunFe (n=1–12)
clusters: a density functional study. J Phys Chem Solids.
2015;76:10–16. DOI:10.1016/j.jpcs.2014.07.022.

[27] Perdew JP, Wang Y. Accurate and simple analytic
representation of the electron-gas correlation energy.
Phys Rev B. 1992;45:13244. DOI:10.1103/PhysRevB.45.
13244.

[28] Soler JM, Artacho E, Gale JD, et al. The SIESTAmethod
for ab initio order-N materials simulation. J Phys: Condens
Matter. 2002;14:2745.

[29] Kleinman L, Bylander DM. Efficacious form for model
pseudopotentials. Phys Rev Lett. 1982;48:1425.

[30] Junquera J, Paz O, Sanchez-Potal D, et al. Numerical
atomic orbitals for linear-scaling calculations. Phys Rev
B. 2001;64:235111.